

**NOAA Technical Report NOS NGS 28**



# **Prediction of Deflections of the Vertical by Gravimetric Methods**

Rockville, Md.  
1984

**U. S. DEPARTMENT OF COMMERCE  
National Oceanic and Atmospheric Administration  
National Ocean Service**

## **NOAA Technical Publications**

# **National Ocean Service/National Geodetic Survey Subseries**

The National Geodetic Survey (NGS), Office of Charting and Geodetic Services, the National Ocean Service (NOS), NOAA, establishes and maintains the basic national horizontal and vertical networks of geodetic control and provides Government-wide leadership in the improvement of geodetic surveying methods and instrumentation, coordinates operations to assure network development, and provides specifications and criteria for survey operations by Federal, State, and other agencies.

NGS engages in research and development for the improvement of knowledge of the figure of the Earth and its gravity field, and has the responsibility to procure geodetic data from all sources, process these data, and make them generally available to users through a central data base.

NOAA geodetic publications and relevant geodetic publications of the former U.S. Coast and Geodetic Survey are sold in paper form by the National Geodetic Information Center. To obtain a price list or to place an order, contact:

National Geodetic Information Center (N/CG17x2)  
Charting and Geodetic Services  
National Ocean Service  
National Oceanic and Atmospheric Administration  
Rockville, MD 20852

When placing an order, make check or money order payable to: National Geodetic Survey. Do not send cash or stamps. Publications can also be charged to Visa, Master Card, or prepaid Government Printing Office Deposit Account. Telephone orders are accepted (area code 301 443-8316).

Publications can also be purchased over the counter at the National Geodetic Information Center, 11400 Rockville Pike, Room 14, Rockville, Md. (Do not send correspondence to this address.)

An excellent reference source for all Government publications is the National Depository Library Program, a network of about 1,300 designated libraries. Requests for borrowing Depository Library material may be made through your local library. A free listing of libraries in this system is available from the Library Division, U.S. Government Printing Office, 5236 Eisenhower Ave., Alexandria, VA 22304 (area code 703 557-9013).

**NOAA Technical Report NOS NGS 28**



# **Prediction of Deflections of the Vertical by Gravimetric Methods**

Rudolf J. Fury

National Geodetic Survey  
Rockville, Md.  
1984

**U. S. DEPARTMENT OF COMMERCE**

Malcolm Baldrige, Secretary

**National Oceanic and Atmospheric Administration**

John V. Byrne, Administrator

**National Ocean Service**

Paul M. Wolff, Assistant Administrator

**Office of Charting and Geodetic Services**

R. Adm. John D. Bossler, Director

For sale by the National Geodetic Information Center, NOAA, Rockville, Md. 20852



# CONTENTS

Preface .....	iv
Abstract .....	1
Introduction .....	1
Geodetic parameter estimation by gravimetric methods .....	1
Computation of mean free-air gravity anomalies .....	3
Error estimation .....	6
Data analysis .....	7
Results of vertical deflection and geoid undulation predictions .....	7
Predicted geodetic parameter entry into the data base .....	8
Acknowledgment .....	8
Credits .....	8
Bibliography .....	23
Appendix A. Recursive relations of Legendre functions .....	24
Appendix B. Linear interpolation of global component of gravity on the geoid .....	24
Appendix C. Geodetic Reference System of 1980 .....	25
Appendix D. Topographic height interpolation .....	25

***Mention of a commercial company or product does not constitute an endorsement by the National Oceanic and Atmospheric Administration***

# PREFACE

A major task in the preparing for the new adjustment of the North American Datum (NAD) is the prediction of deflections of the vertical and geoid undulations at network stations. A system of processes was assembled based on software from the Defense Mapping Agency Aerospace Center (DMAAC). This system employs the numerical integration approach to the Vening-Meinesz and Stokes equations (Schultz et al. 1974, Hopkins and McEntee 1974).

The first successful predictions were achieved at a section of the transcontinental traverse in Indiana (Strange and Fury 1977). The initial version of the converted software was complex. Organization of data reflected early technology, and input/output operations were inefficient. The software subsequently underwent several cycles of redesign in which the system was modified into a unified processor. Gravity anomaly interpolation was substituted by a different method (Schwarz 1978), and organization of data was replaced by more advanced and efficient techniques (Fury 1981). Linkages were established for data flow from the data base (Alger 1978, 1981) to the prediction system (fig. 1), and for the return of predicted deflections into the data base of network stations.

The total system appeared ready for production when concern was expressed about the accuracy of interpolated gravity anomalies via the implemented multiquadric technique. Following experimentation and analysis, the method of least-squares prediction (collocation) was adopted (Hein and Lenze 1979, Goad 1981) and implemented for gravity anomaly interpolation. It was recognized by management that the gravity data holdings of the agency had to be free of gross errors before they could be used for predictions. Therefore, a task group was formed for data editing and quality control, which completed its task in September 1980. A data bank of local gravity anomaly covariance coefficients was subsequently established (Chin 1981) for the interpolation of gravity anomalies in numerical integration. The mean heights of area elements were calculated from the digitized topographic elevations data bank. Three mean anomaly data sets (5'x5', 15'x15', and 1°x1°) were generated over geographic lattices.

The final task of predicting vertical deflections and geoid undulations for the conterminous United States began in October 1980 and was completed in May 1982. The four major processes which were required for the predictions were as follows (fig. 1):

- Network and astronomic stations retrieval from the data base (Query #1).
- Vertical deflections and geoid undulations prediction by gravimetric methods.
- Vertical deflections transformations into the NAD 27 system and error analysis.
- Entry of predicted values into the NGS horizontal data base (Query #2).

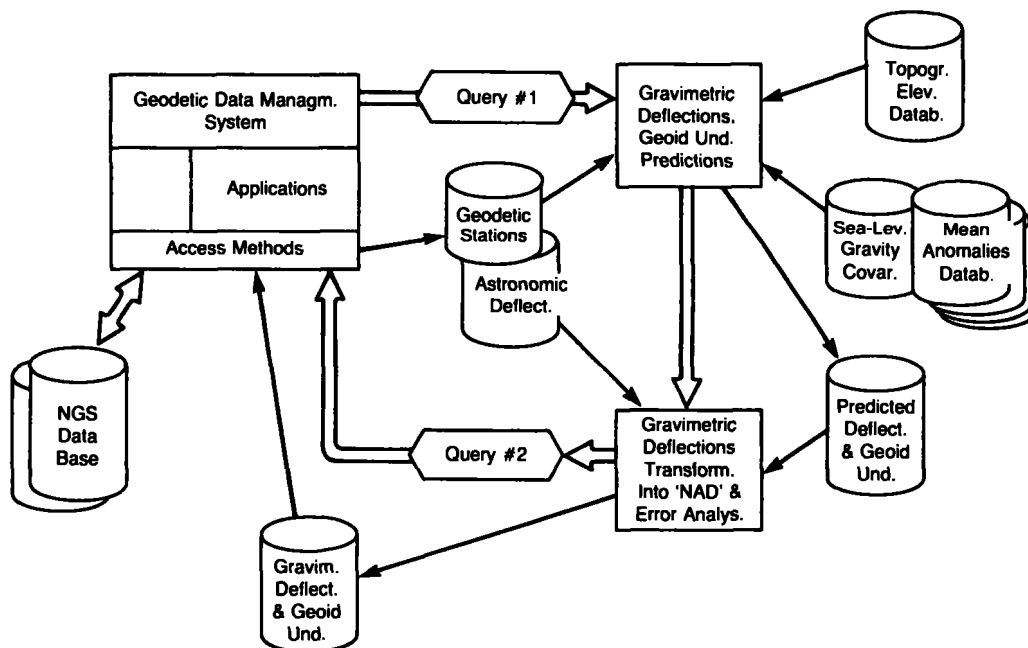


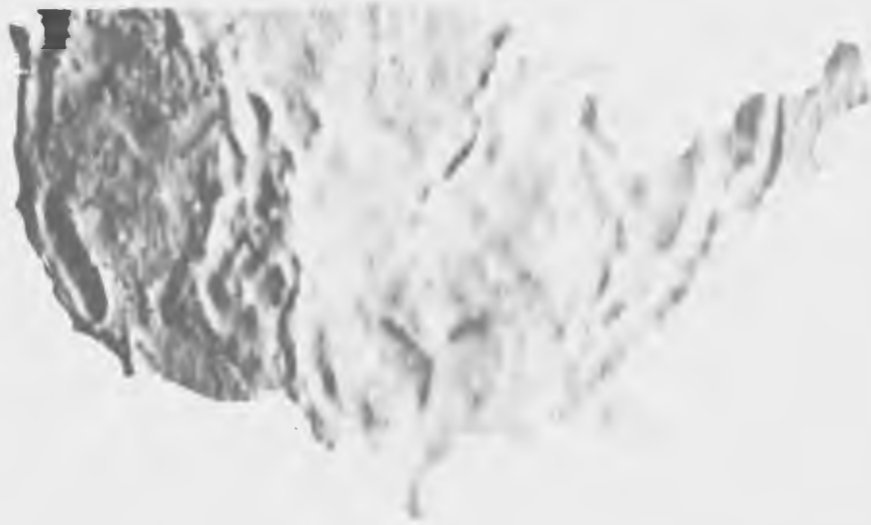
Figure 1. — Gravimetric Deflections and Geoid Undulation Prediction, Error Analysis, and Entry into the NGS Data Base

The flow of data among these processes was complicated because two computer facilities were used. These systems were the IBM 370 and 3033 of Optimum Systems Division of Electronic Data Systems Federal Corporation, Rockville, Maryland which housed the data base, and the IBM 360/195 system of the National Oceanic and Atmospheric Administration (NOAA), which performed the predictions and associated processing. Furthermore, the lack of personnel meant that a very high degree of automation in data management was needed. Consequently, data management procedures were quickly revised and driver modules were redesigned to provide automatic restart and processing recovery capability. In addition, the Asymmetric Multiprocessing feature (networking) of the 360/195 system was fully utilized.

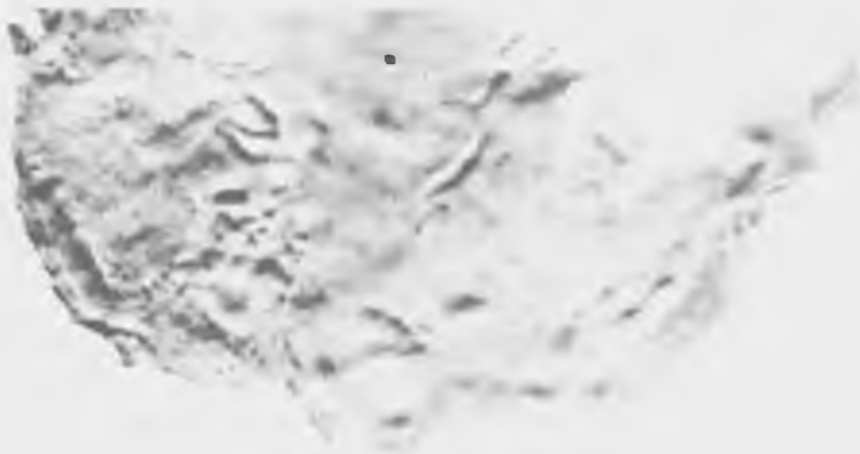
The magnitude of the task can be illustrated by the following statistics:

- Astronomic and network station records were stored on 173 magnetic tape files after retrieval from the data base (35 files hold records for Puerto Rico, Hawaii, and Alaska). The same number (173) of retrieval sessions (jobs) and system utility processor runs were made on the IBM 370 and 3033 systems.
- The geographic area of the conterminous states was divided into 43 area projects for data sets of manageable size. The processing of these projects required the preparation, submittal, editing, and verification of approximately 4,000 prediction runs (computer jobs), 200 to 300 reruns, 150 to 200 transformation and error analysis runs, and the same number of data set backup runs.
- There were 179,980 vertical deflections and geoid undulations predicted and stored in the station records of the data base (some predictions at intersection stations were not entered into the data base). This required the processing and data base entry runs of 43 files corresponding to the area projects.

An indication of the success of the project may be given by the root-mean-square values of deviation between observed and predicted deflections, which were computed to be  $\pm 1.33''$  in the meridional and  $\pm 1.15''$  in the prime vertical components at 3,115 astronomic stations.



Prime vertical components of the deflections of the vertical represented by gray shades, range from (black)  $\leq -8''$  to (white)  $\geq 12''$ , east.



Meridional components of the deflections of the vertical represented by gray shades range from (black)  $\leq -12''$  to (white)  $\geq +6''$ , north.



Undulations of the geocentric geoid represented by gray shades, range from -37 m (black) to -10 m (white).

# PREDICTION OF DEFLECTIONS OF THE VERTICAL BY GRAVIMETRIC METHODS

Rudolf J. Fury  
National Geodetic Survey  
Charting and Geodetic Services, National Ocean Service  
National Oceanic and Atmospheric Administration  
Rockville, MD 20852

## ABSTRACT

Vertical deflections with an accuracy of 1 arc-second are needed at all stations of the National Geodetic Horizontal Network in order to achieve better than 0.5-second accuracy in the reduction of angular measurements. These values will be included in the new adjustment of the North American Datum. Since an abundance of gravity data has become available for the prediction of vertical deflections and geoid undulations to sufficient accuracy, a gravimetric method was developed for predicting these geodetic parameters. This system employs numerical integration of surface gravity in the vicinity of the station and harmonic coefficients of a geoid derived from satellite tracking data in distant areas. The technique was successfully used for the prediction of vertical deflections and geoid undulation at every occupied station of the U.S. horizontal geodetic network. Systematic errors were removed by fitting the predictions to deflections obtained by astronomic methods.

## INTRODUCTION

An early decision in planning for the new adjustment of the North American Datum, to be called the North American Datum of 1983 (NAD 83), specified that deflections of the vertical and geoid undulation were to be associated with every occupied network station in the horizontal data base (Bossler 1978, Strange and Fury 1977). Previously, astronomic deflections had been observed at only 2 percent of the occupied triangulation stations. Similarly, geoid undulation estimates were based on fitting polynomial surfaces to sparsely distributed astrogeodetically determined undulations. Because gravity data have recently become sufficient for geodetic parameter estimation, deflections of the vertical and geoid heights were predicted by gravimetric methods for the remaining 98 percent of the network stations. Following the transformation of vertical deflections into the North American Datum of 1927 (NAD 27) reference system, their standard errors were estimated and the deflections stored, with the predicted geoid heights, in the station records of the horizontal data base of the National Geodetic Survey (NGS). This report describes the computational methodology employed and numerical results achieved in the prediction of parameters for the new adjustment.

## GEODETIC PARAMETER ESTIMATION BY GRAVIMETRIC METHODS

The classical methods of Stokes and Vening-Meinesz have been adopted for the computation of geoid undulations and deflections of the vertical, respectively (Strange and Fury 1977). These geodetic parameters are derived in

a geocentric reference system as defined by the gravity anomalies. To provide for quality control of estimated parameters by direct comparison with astronomically derived values, the deflections of the vertical have been transformed into the NAD 27 geodetic reference system.

### Prediction of Deflections of the Vertical

#### *Deflections on the Geoid*

The integral equation for the calculation of deflections of the vertical is based on the Vening-Meinesz formula (Heiskanen and Moritz 1967)

$$\begin{Bmatrix} \xi \\ \eta \end{Bmatrix} = \frac{1}{4\pi\bar{g}} \iint_{\sigma} \Delta g(\alpha, \psi) \frac{dS(\psi)}{d\psi} \begin{Bmatrix} \cos \alpha \\ \sin \alpha \end{Bmatrix} d\sigma \quad (1)$$

where

$\begin{Bmatrix} \xi \\ \eta \end{Bmatrix}$  = deflection components at a given point on the geoid,

$\iint_{\sigma} \dots d\sigma$  = integration over the global sphere,

$\frac{dS(\psi)}{d\psi}$  = the Vening-Meinesz function, also  $S'(\psi)$

$\Delta g(\alpha, \psi)$  = free-air gravity anomalies on the geoid derived from surface observations,

$\alpha, \psi$  = azimuth and spherical distance of variable point in the integration relative to the given point, and

$\bar{g}$  = the average (global) value of gravity.

The vertical deflection components are represented as the sum of three terms (Strange and Fury 1977)

$$\left\{ \begin{matrix} \xi \\ \eta \end{matrix} \right\} = \frac{1}{4\pi\bar{g}} \int_0^{2\pi} \int_0^{\psi_0} \Delta g^\circ S'(\psi) \begin{Bmatrix} \cos \alpha \\ \sin \alpha \end{Bmatrix} \sin \psi d\psi d\alpha \quad (2)$$

$$+ \frac{1}{4\pi\bar{g}} \int_0^{2\pi} \int_0^{\psi_0} \tilde{\Delta g} S'(\psi) \begin{Bmatrix} \cos \alpha \\ \sin \alpha \end{Bmatrix} \sin \psi d\psi d\alpha + \left\{ \begin{matrix} d\xi \\ d\eta \end{matrix} \right\}$$

The first term expresses the long wavelength (global) components of the deflections which can be obtained using a harmonic series representation ( $\Delta g_n$ ) of the gravity field

$$\Delta g^\circ(\phi, \lambda) = \sum_{n=2}^L \Delta g_n(\phi, \lambda) \quad (3)$$

where  $\Delta g^\circ$  designates boundary (geoid) values, L is the degree of truncation of the series and  $\phi, \lambda$  represent geodetic position. The second term of eq.(2) represents the short wavelength components of the total deflection superimposed on the global field. Therefore, it is computed from the residual gravity anomaly field,

$$\tilde{\Delta g} = \Delta g - \Delta g^\circ \quad (4)$$

where  $\Delta g$  is obtained from observations. Although the integration should be extended over the global sphere in principle, it is limited to a spherical cap ( $0 \rightarrow \psi_0$ ) for practical considerations. The error thus committed is represented by the third term ( $d\xi, d\eta$ ), known as the truncation error.

#### Deflections at Station Height

The vertical deflections calculated via the Vening-Meinesz formula are at the geoid, i.e., mean sea level. These are not directly comparable with astronomically determined (observed) values unless the latter are reduced to the geoid by applying plumb line curvature corrections. However, the calculation of these corrections is involved and the results can be uncertain (Groten 1981). It is better to obtain the vertical deflections at station height. This was accomplished through the extension of the Vening-Meinesz formula to points exterior to the geoid via Pizzetti's generalization of the function  $S'(\psi)$ , (Heiskanen and Moritz 1967: eqs. 6-30, 6-46b). The resulting formula for the short wavelength components of the deflections of the vertical is

$$\left\{ \begin{matrix} \xi \\ \eta \end{matrix} \right\}_s = \frac{1}{4\pi\bar{g}} \int_0^{2\pi} \int_0^{\psi_0} \tilde{\Delta g}(\alpha, \psi) S'(r, \psi) \begin{Bmatrix} \cos \alpha \\ \sin \alpha \end{Bmatrix} \sin \psi d\psi d\alpha \quad (5)$$

where the variable r indicates radial distance from the geocenter to the physical surface, subscript s designates the short wavelength term, and  $\tilde{\Delta g}$  is now computed at the physical surface rather than at the geoid.

#### Prediction of Geoid Undulation

Undulations of the geoid relative to the reference spheroid were calculated by Stokes' formula (Heiskanen and Moritz 1967)

$$N = \frac{R}{4\pi\bar{g}} \iint_{\sigma} \Delta g(\alpha, \psi) S(\psi) d\sigma \quad (6)$$

where N is the geoid undulation,  $S(\psi)$  represents Stokes' function, and  $\Delta g$  are gravity anomalies on the geoid.

In the same fashion as the deflection calculation, the geoid undulation can also be expressed as a sum of three components in which the first term is the global component, and is modeled with a harmonic series similar to the method used for modeling deflections. The second term in the sum is the short wavelength component of the total undulation

$$N_s = \frac{R}{4\pi\bar{g}} \int_0^{2\pi} \int_0^{\psi_0} \tilde{\Delta g}(\alpha, \psi) S(\psi) \sin \psi d\psi d\alpha \quad (7)$$

The third term (dN) represents the truncation error.

#### Computation of Global Components of the Parameters

A set of spherical harmonic coefficients (truncated GEM-10), was chosen to calculate the global components (Strange and Fury 1977) of the parameters

$$\xi_g = \frac{1}{R\gamma} \frac{GM}{r} \sum_{n=2}^L \left(\frac{a}{r}\right)^n \sum_{m=0}^n [(\bar{C}_n^m - \bar{C}_n^{\circ}) \cos(m\lambda) + \bar{S}_n^m \sin(m\lambda)] \frac{d\bar{P}_n^m(\sin\phi)}{d\phi} \quad (8)$$

$$\eta_g = \frac{1}{R\gamma \cos\phi} \frac{GM}{r} \sum_{n=2}^L \left(\frac{a}{r}\right)^n \sum_{m=0}^n [-(\bar{C}_n^m - \bar{C}_n^{\circ}) \sin(m\lambda) + \bar{S}_n^m \cos(m\lambda)] m \bar{P}_n^m(\sin\phi) \quad (9)$$

$$N_g = \frac{1}{\gamma} \frac{GM}{r} \sum_{n=2}^L \left(\frac{a}{r}\right)^n \sum_{m=0}^n [(\bar{C}_n^m - \bar{C}_n^{\circ}) \cos(m\lambda) + \bar{S}_n^m \sin(m\lambda)] \bar{P}_n^m(\sin\phi) \quad (10)$$

where,  $\xi_g, \eta_g, N_g$  are the deflections of the vertical and geoid undulation, respectively,

GM = product of gravitational constant and mass of the Earth,

$\gamma$  = normal gravity at latitude,

r = radial distance to geoid,

a = mean equatorial radius of the Earth

$\bar{P}_n^m(\sin\phi)$  = spherical harmonic (Legendre) functions (normalized),

$\frac{d\bar{P}_n^m(\sin\phi)}{d\phi}$  = derivatives of harmonic functions,

$\bar{C}_n^m, \bar{S}_n^m$  = coefficients of spherical harmonic expansion (normalized),

$\bar{C}_n^{\circ}$  = coefficients of reference field which are functions of flattening ( $\bar{C}_n^{\circ} \neq 0$  only for  $n=2$  and  $n=4$  to an accuracy of 4th power in the second eccentricity), and

L indicates the degree of truncation ( $L=22$ ) for computations in eq. (8), (9) and (10).

The normalized Legendre functions and their deriva-

tives were calculated recursively through the relations given in appendix A.

A remark is appropriate concerning the computation of the radial distance ( $r$ ) to the geoid. This value is

$$r = R + N$$

where  $R$  is the radial distance to the spheroid and  $N$  is the geoid undulation. However,  $N$  is initially not known. Therefore, the evaluation of double sums, i.e., eq.(10), is iterated with  $N=0$  initially. Convergence is usually reached in two iterations.

As indicated, the double sums are evaluated first to obtain the global components of the deflections of the vertical and geoid undulation at network stations. However, they are also utilized in calculating the gravity reference field, i.e., eq. (3). When performed many times, the evaluation of the double sums is a time consuming computation, even though the algorithm was optimized as much as possible. The large number of computations is necessitated by the need to calculate gravity anomaly residuals ( $\Delta g$ ) at a large number of area elements when integrating over the spherical cap for short wavelength components, using eqs. (5) and (7), as will be discussed in the next section.

Since the gravity field produced by the satellite-derived spherical harmonic model is smooth, point anomalies on the geoid were calculated only at five locations in the vicinity of the station through the harmonic series

$$\Delta g^o = \frac{GM}{r^2} \sum_{n=2}^L (n-1) \left(\frac{a}{r}\right)^n \sum_{m=0}^n [(\bar{C}_n^m - \bar{C}_n^o) \cos(m\lambda) + \bar{S}_n^m \sin(m\lambda)] \bar{P}_n^m(\sin\phi) \quad (11)$$

These five reference values then provided the basis for linear interpolation of anomalies at other points on the geoid. (See appendix B.)

### Computation of Short Wavelength Components of the Parameters

The practical evaluation of the integrals for the short

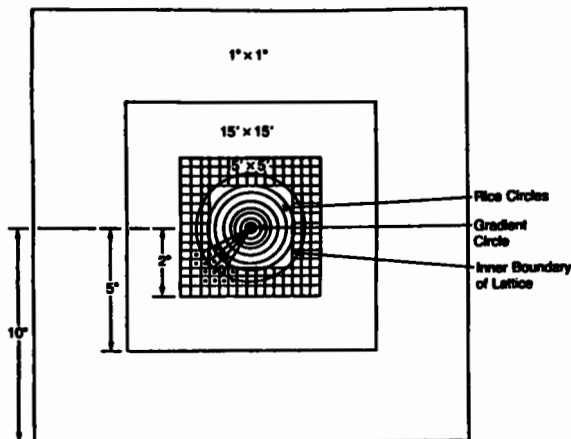


Figure 2. —Gravity Anomaly Integration Scheme

wavelength terms is achieved through numerical integration. An important consideration in such calculations is the subdivision of the spherical cap (i.e., integration region in the vicinity of the stations) into area elements. The method chosen is a combination of circular sectors [Rice-circles (Rice 1952)] and geographic quadrangles (see fig. 2.) In the immediate vicinity of the station (0 - 235 meters), a gradient circle is used to evaluate the effect of the gravity field (Schultz et al. 1974). From this circular area (Rice-ring no. 5) to 45' in latitude and 45'/cos $\phi$  in longitude (Rice-ring no. 42) the mean anomalies ( $\Delta \tilde{g}$ ) of circular sectors are calculated by averaging the interpolated values at sector corners. The remaining area of the spherical cap ( $\psi=10^\circ$ ) is divided into three concentric zones over a geographic lattice formed by meridional and parallel spherical arcs: the first zone extending from the circular sectors out to 2° from the station is overlaid with 5'x5' blocks, from this boundary to 5° with 15'x15' blocks, finally to 10° with 1°x1° blocks. The mean anomalies ( $\Delta \tilde{g}$ ) for this geographic lattice were precalculated using observed values from the NGS gravity data bank. There is a small error committed in matching the circular outer boundary of sectors with the rectangular inner boundary of geographic lattice. This error is minimized by first moving the rectangular boundary to the even 5' grid line in the vicinity of outermost circle (i.e., 45' from the station in latitude and 45'/cos $\phi$  in longitude); secondly, the summation includes only those sectors whose center points fall within this rectangular area (fig. 2). The truncation limit ( $\psi=10^\circ$ ) was chosen as a compromise between the goal for achievable accuracy ( $\pm 1''$ ) and computational cost (Bossler 1978). The global harmonic geoid model used in the computations (GEM-10) was truncated to  $L=22$  for computational economy. Considering that the estimated resolution of this harmonic model in terms of wavelength is  $360^\circ/22 \approx 16^\circ$ , the spherical cap radius should have been  $16^\circ$ . However, the moderate gain in accuracy (Strange and Fury 1977, fig. 2) versus the very significant increase in computational cost did not justify the effort.

### COMPUTATION OF MEAN FREE-AIR GRAVITY ANOMALIES

Mean free-air gravity anomalies have been computed for the solution of the Stokes and Vening-Meinesz integrals. Since the long wavelength components of geodetic parameters were calculated directly from harmonic series, mean anomalies are needed for the calculation of short wavelength components only. Further, the short wavelength components are superimposed on the global model, which implies a residual gravity field for numerical integration. The appropriate mean anomaly residuals are then

$$\tilde{\Delta g} = \Delta g - \sum_{n=2}^L \Delta g_n \quad (12)$$

where  $\Delta g$  represents mean anomalies calculated from observations.

**Geodetic Reference Field**

The point free-air anomalies stored in the NGS gravity data bank have been computed on the Geodetic Reference System 1967 (GRS1967)

$$\Delta g(\phi, \lambda) = g(\phi, \lambda) - \gamma(\phi, \lambda) \quad (13)$$

where  $g(\phi, \lambda)$  is an observed value reduced to mean sea level (geoid), and  $\gamma(\phi, \lambda)$  is the theoretical (normal) gravity at the surface of the spheroid. The spheroid parameters are

$$\begin{aligned} GM &= 0.398603 \times 10^{15} \text{ cm}^3/\text{sec}^2 \\ a &= 6378160 \text{ m} \\ \omega &= 0.72921151467 \times 10^{-4} \text{ rads/sec} \\ J_2 &= 1082.7 \times 10^{-6} \text{ (exact) } [J_2 = -\bar{C}_2^0] \end{aligned}$$

Derived parameters:  $J_4 = -2.3712644 \times 10^{-6}$   
 $\gamma_e = 0.97803187 \times 10^6 \text{ mgal}$   
 $1/f = 298.2472$

where  $\omega$  is the angular velocity of the earth,  $1/f$  is the reciprocal flattening of the spheroid,  $\gamma_e$  is the equatorial normal gravity, and the other symbols have already been identified.

The GRS1967 constants were substituted into the harmonic series (eqs. 8, 9, 10, 11). As a result, the long wavelength components of the parameters are then referenced to this field (i.e.,  $\bar{C}_2^0 - \bar{C}_2^0 = \bar{C}_4^0 - \bar{C}_4^0 = 0$ ). It was desirable to obtain the geoid undulations as close as possible to the GRS80 system planned by NGS for geometric reference. However, since no final parameters were yet adopted, the following zonal terms (normalized) were substituted into the harmonic series

$$\begin{aligned} \Delta \bar{C}_2^0 &= \bar{C}_2^0(\text{GEM-10}) - \bar{C}_2^0(\text{GRS1967}) = +0.340074 \times 10^{-7} \\ \Delta \bar{C}_4^0 &= \bar{C}_4^0(\text{GEM-10}) - \bar{C}_4^0(\text{GRS1967}) = -0.253549 \times 10^{-6} \end{aligned} \quad (14)$$

Some very small effects seep into the higher harmonic terms by this substitution due to weak correlations. Since the harmonic coefficients of GEM-10 have been derived from least-squares solution, they are not entirely independent, i.e., orthogonality relations are not perfect.

The computed geoid undulations (full value) were compared with values derived from Doppler tracking data at 10 stations (table 1). Geoid undulations determined by Doppler tracking were transformed into the GRS80 system (appendix C). The test stations are well distributed in the conterminous United States. Agreements of the two sets of values indicate that the substitution of  $\Delta \bar{C}_2^0$  and  $\Delta \bar{C}_4^0$  was appropriate.

**Observed Gravity Reduction**

Free-air anomalies on the geoid (boundary values) are needed for the solution of the third boundary-value problem of physical geodesy, i.e., the prediction of geoid undulation. Free-air anomalies at the physical surface are also needed for the computation of the disturbing potential (Heiskanen and Moritz 1967: 233) and for its derivatives, i.e., deflections of the vertical at station height (Heiskanen and Moritz 1967: 235). When surface anomalies are corrected for the effect of the terrain, the formalization becomes equivalent to the solution of Molodensky's boundary-value problem, assuming that free-air anomalies are linearly correlated with topographic elevations. In giving a physical interpretation to such solution, Moritz (1968: 35) shows its relation to the disturbing potential of a surface layer which may be obtained through the "condensation reduction" of Helmert (Heiskanen and Moritz 1967: 145). A "co-geoid" surface thus defined is a "single-layer free-air geoid" (Bjerhammar 1967), which is obtained when all masses of topography are condensed in a layer at mean sea level. A significant feature of this co-geoid is the fact that to a linear approximation the predicted deflections of the vertical are invariant with respect to the condensation of topographic masses.

The masses to be removed were estimated via a Bouguer plate using the topographic height of the gravity station for plate thickness and a density ( $\rho$ ) of 2.67 g/cm<sup>3</sup>. Corrections were applied for the deviations of topography from the Bouguer plate (Goad 1981). The planar (infinite) Bouguer plate approximation to the topographic masses carries a significant error (Moritz 1968), but this is of no great consequence in this application since its utility is limited to the smoothing of the gravity field for interpolation.

**Table 1. — Comparison of geoid undulations predicted by gravimetric methods and computed from Doppler satellite tracking**

Sta.	Latitude ° ' "	Longitude ° ' "	H (m)	Doppl. N(m)	Pred. N(m)	Diff. (m)
10028	30 34 4.34	86 12 58.92	36.00	-26.46	-26.37	-0.09
10055	37 29 53.63	122 29 50.24	53.82	-33.57	-33.19	-0.38
10070	47 7 16.58	122 29 20.36	95.21	-22.45	-23.52	+1.07
51041	41 38 26.87	101 35 56.21	1179.40	-19.98	-20.44	+0.46
51057	40 23 42.05	115 12 25.13	1856.00	-20.23	-19.76	-0.47
51081	46 18 30.44	85 27 23.69	260.62	-36.34	-36.62	+0.28
53114	38 26 13.65	79 49 55.37	822.26	-30.65	-29.88	-0.77
51134	32 51 55.56	117 14 59.06	76.21	-37.58	-37.18	-0.40
51960	39 8 16.36	123 12 38.69	197.92	-30.69	-30.61	-0.08
51014	27 57 25.32	80 33 28.02	7.26	-30.16	-29.81	-0.35

Following the removal of masses the observation ( $g$ ) was reduced to sea level using the uniform free-air gradient of 0.3086 mgal/meter,

$$\Delta g(\phi, \lambda)^s = g(\phi, \lambda, h) - A_i + 0.3086h - \gamma(\phi, \lambda) \quad (15)$$

where  $\Delta g(\phi, \lambda)^s$  = gravity anomaly at sea level,

$g(\phi, \lambda, h)$  = observed gravity at station,

$A_i$  = the effect of removed masses,

0.3086h = reduction from station height to sea level in free space, and

$\gamma(\phi, \lambda)$  = gravity at the spheroid.

The condensation reduction of Helmert may be viewed as a limiting case of isostatic reduction of the Pratt-Hayford type when the depth of condensation ( $D$ ) is zero (Heiskanen and Moritz 1967: 145). Accordingly,

$$\Delta g(\phi, \lambda) = \Delta g(\phi, \lambda)^s + A_c \quad (16)$$

in which  $A_c$  represents the effect of restored topography calculated with constant density ( $\rho = 2.67\text{g/cm}^3$ ) considering the fact that  $A_i$  was obtained through a Bouguer reduction (Heiskanen and Moritz 1967: 138). The "direct effect" ( $-A_c + A_i$ ) is a small quantity since "the attraction of the Helmert layer nearly compensates that of the topography" (Heiskanen and Moritz 1967: 145),

$$A_i = 2\pi G\rho h_P \approx A_c = 2\pi G\rho \bar{h} \quad (17)$$

where  $h_P$  represents the topographic height of gravity station,  $\bar{h}$  is the mean height of template compartments derived from the digitized topographic heights. The value of  $\bar{h}$  can be set to the station height as an option; as a result a topography of constant thickness could be compressed into the surface layer.

Mean anomalies were precomputed for the geographic lattice from data in the NGS gravity observations data bank. Three data sets were generated for  $5^\circ \times 5^\circ$ ,  $15^\circ \times 15^\circ$ , and  $1^\circ \times 1^\circ$  geographic blocks. These anomalies were considered boundary values on the co-geoid, i.e.,

$$\Delta g(\phi, \lambda) = g(\phi, \lambda, h) + 0.3086h - \gamma(\phi, \lambda) \quad (18)$$

since the direct effect may be neglected in the distant zones. Because the indirect effect of condensation reduction is even smaller than the direct effect (e.g., 1m per 3km of average topographic height) its estimation was not considered.

The condensation anomalies may be regarded as sea-level, free-air anomalies which could have been obtained by linear approximation of downward continuation of surface gravity anomalies (Heiskanen and Moritz 1967: 329). This implies that "modern" methods of physical geodesy are applicable in computing deflections of the vertical at the physical surface. Indeed, this reasoning was followed in calculating deflections of the vertical at station height (Heiskanen and Moritz 1967: 320).

#### Gravity Anomaly Interpolation

Although there is an abundance of gravity in most areas of the United States, sizeable gaps or areas with

sparse coverage still remain. Therefore, interpolation and extrapolation (prediction) are basic requirements in parameter estimation.

Least squares collocation has been used successfully for gravity anomaly predictions and error estimation (Tscherning 1975). The method of least squares collocation for the prediction of gravity anomalies ( $\Delta g_p^s$ ) and their error variances ( $\sigma_{\Delta g_p^s}^2$ ) are represented by the formulae (Lachapelle 1978)

$$\Delta g_p^s = \bar{C}_{\Delta g^s, \Delta g_p^s}^T \cdot [C_{\Delta g^s, \Delta g^s}]^{-1} \cdot \bar{\Delta g}^s \quad (19)$$

$$\sigma_{\Delta g_p^s}^2 = \sigma_{\Delta g^s}^2 - \bar{C}_{\Delta g^s, \Delta g_p^s}^T \cdot [C_{\Delta g^s, \Delta g^s}]^{-1} \cdot \bar{C}_{\Delta g^s, \Delta g_p^s} \quad (20)$$

where  $\bar{\Delta g}^s$  is a vector of the gravity anomalies derived from observations ("observed" gravity  $\Delta g(\phi, \lambda)^s$  was "centered" on a reference plane);  $[C_{\Delta g^s, \Delta g^s}]$  represents a covariance matrix of observed anomalies,  $\bar{C}_{\Delta g^s, \Delta g_p^s}$  is the cross-covariance (column) vector between observed and predicted anomalies, and  $\sigma_{\Delta g^s}^2$  designates the variance of prediction. The covariance function of gravity anomalies was defined in terms of Legendre polynomials (Heiskanen and Moritz 1967, Goad 1981)

$$C(\Delta g_{Q, \tau}^s, \Delta g_{\tau, Q}^s) = C(\psi_{Q, \tau}) = \sum C_n \left[ \frac{R_b}{r_Q r_\tau} \right]^{n+2} P(\psi_{Q, \tau})_n \quad (21)$$

where the  $C_n$  are degree variances,  $r_Q$  and  $r_\tau$  are geocentric radii to points Q and T, and  $R_b$  is the radius of Bjerhammar sphere. The value of  $C_n$  was calculated from Goad (1981)

$$C_n = \frac{(n-1)^2}{R_b^2} K_n$$

where

$$K_n = \left( \frac{GM}{R_b} \right)^2 \frac{10^{-10}(2n+1)}{n^4} e^{2\alpha n}$$

and

$$\alpha = 0.876 \times 10^{-4}$$

This method of prediction is most applicable to a field of smooth anomalies. Therefore, the vector of observed anomalies ( $\bar{\Delta g}^s$ ) was defined as "sea level anomalies" which are identical to "refined Bouguer-anomalies" (i.e., terrain corrected) on land (Heiskanen and Moritz 1967), and free-air anomalies on oceans (i.e.,  $h=0$ ).

A data bank of prediction coefficients given by the product  $[C_{\Delta g^s, \Delta g_p^s}]^{-1} \cdot \bar{\Delta g}^s$  is stored for predicting sea level anomalies at any point. The continental United States was partitioned into  $1^\circ \times 1^\circ$  geographic quadrangles. Each quadrangle was further subdivided into four  $30' \times 30'$  sectors for the calculation of local anomaly covariances. The prediction coefficients represent the sea-level anomaly surfaces within the sector boundaries. This requires the storage of a large number of coefficients for large numbers of observations. The problem was solved by iterative selection of those observed anomalies that significantly contributed to predicted sea-level anomalies. The maximum prediction error could there-

fore be kept to any desired level by storing a sufficient number of covariances for the sector. The iterative selection of data reduced the number of covariances to be stored by 30 to 60 percent.

### Topographic Height Interpolation

The mean heights of area elements in the numerical integration were obtained through the average point elevations at circular sector corners. The point elevations were computed via three-point interpolation from the NGS digitized topographic data bank. This data set contains a point elevation for every 30 seconds of latitude and longitude in the United States, extending into Canada, Mexico, and the oceans. The heights were computed from the three closest digitized values forming a triangle (appendix D).

## ERROR ESTIMATION

The possibility of estimating geodetic parameter errors rigorously through error propagation was investigated and judged to be too complex. Testing indicated that it was not feasible to compute the errors by this method. A practical solution was implemented which consisted of comparing the predictions with values derived from observations.

### Transformation of Deflection Components

The predicted deflections of the vertical are referenced to the modified GRS1967 system and are not directly comparable to the astronomically derived values

$$\begin{aligned}\xi_A &= \Phi - \phi \\ \eta_A &= (\Lambda - \lambda) \cos \phi\end{aligned}\quad (22)$$

where  $\xi_A, \eta_A$  are the astrogeodetic deflection components,  $\Phi, \Lambda$  are astronomic latitude and longitude, respectively, and  $\phi, \lambda$  are the corresponding geodetic values which are referenced to the North American Datum of 1927. For the purpose of direct comparison, the predicted values were transformed into the NAD 27 system via differential transformation ( $\lambda$  positive east).

$$\begin{aligned}\delta\xi &= -\frac{1}{M+H}[-\sin\phi\cos\lambda\delta u - \sin\phi\sin\lambda\delta v + \cos\phi\delta w \\ &+ a e^2 \frac{\cos 2\phi(1-e^2\sin^2\phi) + e^2\sin\phi\cos\phi}{(1-e^2\sin^2\phi)^{3/2}} \\ &(\cos\lambda\delta\psi - \sin\lambda\delta\epsilon) \\ &+ \frac{e^2\sin\phi\cos\phi}{(1-e^2\sin^2\phi)^{1/2}}\delta a \\ &+ \sin\phi\cos\phi(2N+e^2M\sin^2\phi)(1-f)\delta f]\end{aligned}\quad (23)$$

$$\delta\eta = -\frac{1}{(N+H)\cos\phi}[-\cos\phi\sin\lambda\delta u + \cos\phi\cos\lambda\delta v -$$

$$Ne^2\sin\phi\cos\phi(\sin\lambda\delta\psi + \cos\lambda\delta\epsilon)]$$

where

$$e^2 = \frac{e^2}{1-e^2}; \quad N = \frac{a}{(1-e^2\sin^2\phi)^{1/2}}; \quad M = \frac{a(1-e^2)}{(1-e^2\sin^2\phi)^{3/2}}$$

$\delta u, \delta v, \delta w$  indicate shifts of ellipsoid (i.e. geocentric-geodetic),

$\delta a, \delta f$  are corrections to semimajor axis and flattening,

$\delta\epsilon, \delta\psi, \delta\omega$  are differential rotations,

$a, e$  are the semimajor axis and eccentricity of reference system,

$M, N$  are radii of spheroidal curvature in the meridian and prime vertical, respectively,

$h$  is the geodetic height of station

$\delta\xi, \delta\eta$  are corrections to transform geodetic into geocentric deflection components

The gravimetrically predicted vertical deflections in the NAD 27 system are then

$$\begin{aligned}\xi_{NAD} &= \xi_{GRS67} - \delta\xi \\ \eta_{NAD} &= \eta_{GRS67} - \delta\eta\end{aligned}\quad (24)$$

The following constants were used in the differential transformation (Vincenty 1976)

$$\begin{aligned}a(\text{NAD27}) &= 6378206.4 \text{ m} \\ 1/f(\text{NAD27}) &= 294.9787 \\ \delta u &= -22 \text{ m} \\ \delta v &= +157 \text{ m} \\ \delta w &= +176 \text{ m}\end{aligned}$$

The predicted geoid undulations are already very close to the GRS80 system (table 1) adopted as preliminary reference for the geodetic network. Therefore, any further corrections may be applied regionally.

### Interpolation and Error Estimation of Parameters

The general approach to quality control and error estimation was heuristic in nature due to the large computational effort which would have been required for error propagation. Assuming that the parameters derived from observations have very small errors as compared to prediction, any difference between predicted and observed values are attributed to errors in prediction. Therefore, the predicted values must be corrected to match the observations. A weighted interpolation scheme was adopted which has the characteristic of predicting the observed values at control stations. It is similar to astrogravimetric leveling (Heiskanen and Moritz 1967: 203), but it is not limited to a profile. Instead, any number of observed parameters may be utilized. The interpolated parameters are then

$$\left\{ \begin{matrix} \xi \\ \eta \\ N \end{matrix} \right\}_P = \left\{ \begin{matrix} \xi \\ \eta \\ N \end{matrix} \right\}_P + \frac{1}{\sum w} \sum_{m=1}^M \left( \left\{ \begin{matrix} \xi \\ \eta \\ N \end{matrix} \right\}_m^\sigma - \left\{ \begin{matrix} \xi \\ \eta \\ N \end{matrix} \right\}_P \right) w_m \quad (25)$$

where the superscripts  $\sigma$  and  $p$  indicate observed and predicted values, respectively, the subscripts  $P$  designate interpolated stations, while  $m$  designates the control stations. The weights ( $w$ ) were chosen as the inverse

distances between predicted and control station; the summation limit was variable.

The errors of interpolated parameters were computed from two sources of information. The standard errors of observed values at control stations were summed with the weighted average of deviations

$$\sigma(\xi, \eta, N)_P = \left[ \frac{1}{M} \sum_{m=1}^M \sigma^2(\xi, \eta, N)_m^A + \frac{1}{(\sum w)^2} \sum_{m=1}^M w_m^2 \Delta^2(\xi, \eta, N) \right]^{1/2} \quad (26)$$

where the  $\sigma$  indicates error estimates, the A superscript designates standard error for astronomic or Doppler observations,  $\Delta$  is the residual difference between observed and predicted values following a regional correction (bias) to the latter, i.e., interpolated among neighboring control stations.

### DATA ANALYSIS

The unified parameter estimation system was first tested in a topographically undisturbed area with dense gravity coverage. Consequently, the prediction method was expected to give optimal results, thus revealing errors in the code (Strange and Fury 1977). Following the removal of regional distortions (biases), root mean square (RMS) values of residual differences ( $\Delta$ ) were  $\pm 0.43''$  in  $\xi$  and  $\pm 0.41''$  in  $\eta$  from 25 stations. Another test for 22 stations in the topographically rugged New Mexico test area produced  $\pm 1.951''$  in  $\xi$  and  $\pm 2.852''$  in  $\eta$ . However, the distribution of gravity data was sparse and did not sample the gravity field adequately in the New Mexico area. In addition, some new software features were incomplete. A second test in this same area was performed with the latest version of the prediction system in which 441 astronomic deflections were compared with the predicted values following corrections for regional distortions. The gravity sampling was improved by obtaining additional data. The digitized topographic elevations in the NGS data bank were also utilized. The regional biases were  $-0.42''$  and  $-0.64''$  in the prime vertical and meridional components, respectively. The RMS residual differences were  $\pm 0.92''$  in  $\xi$  and  $\pm 1.06''$  in the  $\eta$  components; the distribution of estimated prediction errors is given in table 2.

**Table 2. —Distribution of estimated errors in New Mexico**

Error intervals (arc seconds)	$\sigma_\xi$ per cent	$\sigma_\eta$ per cent
$\pm 0.0 - 0.5''$	73	60
$\pm 0.5 - 1.5''$	24	33
$\pm 1.5 - 2.5''$	3	1

Some remarks are appropriate concerning these results. It was mentioned in the discussion of the computation of

condensed masses (eq. 17) that the mean heights of compartments could be set to the station height, in which case the masses equivalent to a uniform Bouguer plate are restored. The predictions should be corrected then by adding the relative effect of topography, computed separately. NGS tested this approach and the results improved, although not dramatically (approximately 8 percent). The computation of topographic effects separately consumed extra processing time and resources which were almost equivalent to the prediction effort. Consequently, considering the goal of  $\pm 1''$  accuracy in predicted parameters (Bossler 1978), which could be achieved even over an area with significant topography, this latter option was not exercised. This significantly shortened the project life and saved valuable computational resources. Further improvement in prediction accuracy can be achieved by reducing the truncation error in numerical integration by modifying the Stokes and Vening-Meinesz kernels (Fell and Karaska 1981, Hagiwara 1973).

### RESULTS OF VERTICAL DEFLECTION AND GEOID UNDULATION PREDICTIONS

Figure 3 shows the geographic distribution of 179,980 network stations at which deflections of the vertical and geoid undulations were predicted. Similarly, figure 4 displays the distribution of astronomic stations within the conterminous United States. The latter indicates that the spacing of astronomic stations is inadequate to estimate the local variability of deflections, but can be used to remove regional distortions from the gravimetrically predicted deflections. The bar charts in figures 5, 6, and 7 give the statistical distributions of observed vertical deflections and Doppler-system derived geoid undulations. These have been compared to the predicted values for the calculation of regional distortions in the sampled gravity field. The distortions, of which distributions are shown in figures 8, 9, and 10, represent "calibration" values with which the predictions should be corrected to obtain deflections and geoid undulations in the respective reference system. A few large values suggest that the sampling of the gravity field at some regions is inadequate.

Some measure of the success of geodetic parameters prediction in the conterminous States was sought. The accuracy indicators could not be obtained by the regular computations of "calibrating" the predicted values at astronomic and Doppler stations because the interpolation method reproduces the observed values, i.e., the residual differences would be zero. Therefore, the observations were assumed unknown at the test stations, so that only surrounding values were used in interpolation for comparing observed and predicted deflections and geoid undulations. This approach for obtaining accuracy indicators is clearly inconsistent with the principles of the interpolation technique used and tends to produce

pessimistic estimates. Nevertheless, it provides a reasonable measure of the success of parameter estimation. The results of this test are given in figures 11, 12, and 13, which show the test results for the meridional and prime vertical components and for geoid undulations. Accordingly, the RMS of residual differences at astronomic stations was  $\pm 1.33''$  in the meridian and  $\pm 1.15''$  in the prime vertical components and  $\pm 1.40$  meters in geoid undulations. The residual differences  $[\Delta(\xi, \eta, N)]$  were also substituted into the formula for computing error estimates of predicted geodetic parameters.

Figures 14 through 19, as well as tables 3 and 4, show the results of a production subproject. The boundaries of the prediction area were from  $44^\circ$  to  $46^\circ$  in latitude, and from  $116^\circ$  to  $125^\circ$  in longitude. The regional bias was  $1.91''$  in the meridian and  $0.85''$  in the prime vertical. The RMS of residual differences at 42 control stations was  $1.05''$  in the meridian, and  $0.93''$  in the prime vertical components (figs. 16 and 17). Figures 18 and 19 show the distribution of estimated errors.

Figures 20 through 30 demonstrate the problems that occurred in areas where the gravity field sampling was inadequate. The distributions of 141 astronomic observations in the area of  $\phi = 39^\circ - 44^\circ$  and  $\lambda = 116^\circ - 125^\circ$  are shown in figures 20 and 21. There were 85 stations used as astronomic control; for these the regional distortions are shown in figures 22 and 23; The corresponding RMS of residual differences is  $\pm 1.24''$  in the meridian and  $\pm 1.66''$  in the prime vertical (figs. 24 and 25). Finally, figures 26 and 27 show the distributions of estimated errors for 5,526 predicted deflections. It is immediately recognizable on figures 22 and 23 that one regional distortion is excessively large in each component which is at the same control station. Since the estimated standard errors of the astronomic observations are  $0.3-0.7''$ , the predicted value is suspected to be in error. This supposition is confirmed by the gap in the gravity data distribution shown in figure 28, where the position of the station is indicated. Therefore, this station was dropped as a control station (i.e., the regional distortion correction was considered unreliable). The recomputed RMS of residual differences at astronomic stations dropped to  $\pm 1.19''$  in the meridian and  $\pm 1.33''$  in the prime vertical components. Figures 29 and 30 show the distribution of recomputed prediction errors.

#### **PREDICTED GEODETIC PARAMETER ENTRY INTO THE DATA BASE**

Deflections of the vertical and geoid undulations were predicted at 179,980 network stations. These also include

the collocated astronomic stations. The data base entry records contained the following information:

- Quad identifier (QID)
- Quad station number (QSN)
- Predicted vertical deflection in the meridian
- Estimated error of meridian component
- Predicted vertical deflection in prime vertical
- Estimated error of prime vertical component
- Predicted geoid undulation
- Time stamp #1 — date and time of prediction
- Time stamp #2 — date and time of error analysis and estimation
- Model code #1 — indicates parameters of gravity reference field (GRS67)
- Model code #2 — indicates transformation parameters (GRS67 to NAD 27)

Figures 31 and 32 show distributions of the predicted vertical deflections, and figures 33 and 34 show the estimated errors. The predicted values are identical with the astronomically observed deflections at control stations, but they are different from the astronomically derived values when the regional distortion at an astronomic station was judged unreliable and not used in the interpolation. These areas will have to be reviewed. Interpolation and error analysis were not performed for geoid undulations prior to data base entry since control data were not available at the appropriate time.

#### **ACKNOWLEDGMENT**

It is a pleasant duty to express appreciation to William C. Strange of NGS who provided technical advice and consultation in the developmental stage of the project. The advice of F. Foster Morrison, Clyde C. Goad, Allen J. Pope, and Tomas Soler, also of NGS, is gratefully acknowledged. Technical discussions with Christian Tscherning of the Danish Geodetic Institute are also gratefully acknowledged.

#### **CREDITS**

Clyde C. Goad designed the collocation system for gravity interpolation and formulated the modified astrogravimetric interpolation.

Charles R. Schwarz designed the data compression algorithms for the digitized topographic data bank and investigated error propagation.

Tomas Soler derived the differential transformations for the deflections of the vertical.



Figure 3. — Geographic Distribution of Network Stations

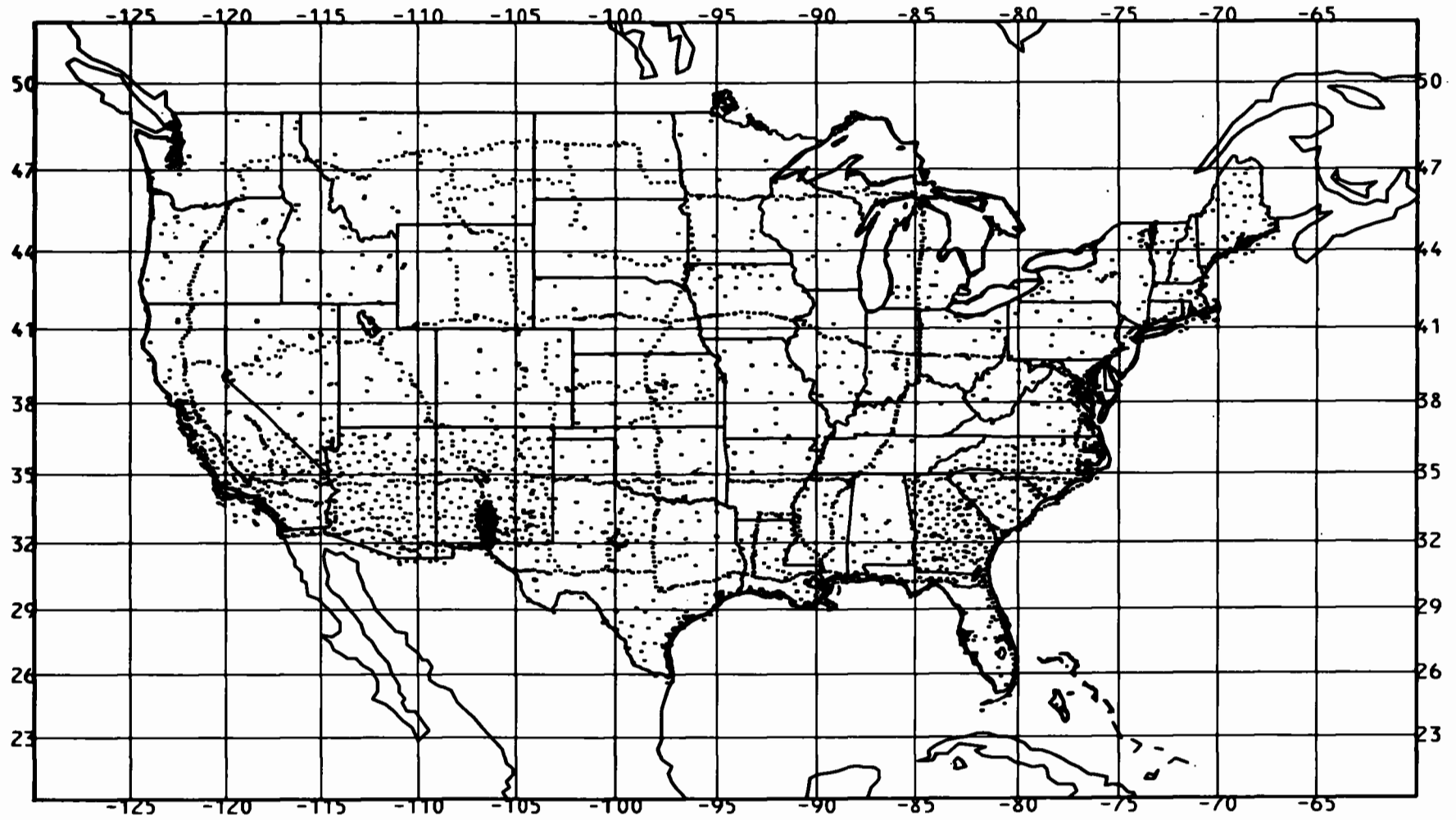


Figure 4. — Geographic Distribution of Astronomic Stations



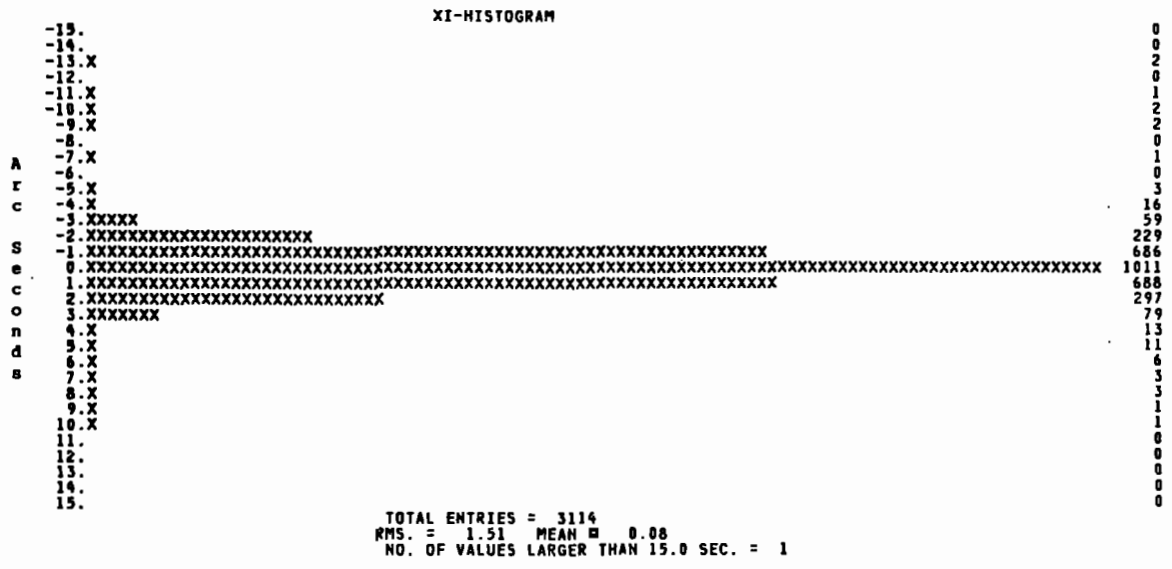


Figure 8. —Distribution of Regional Distortions in the Meridian

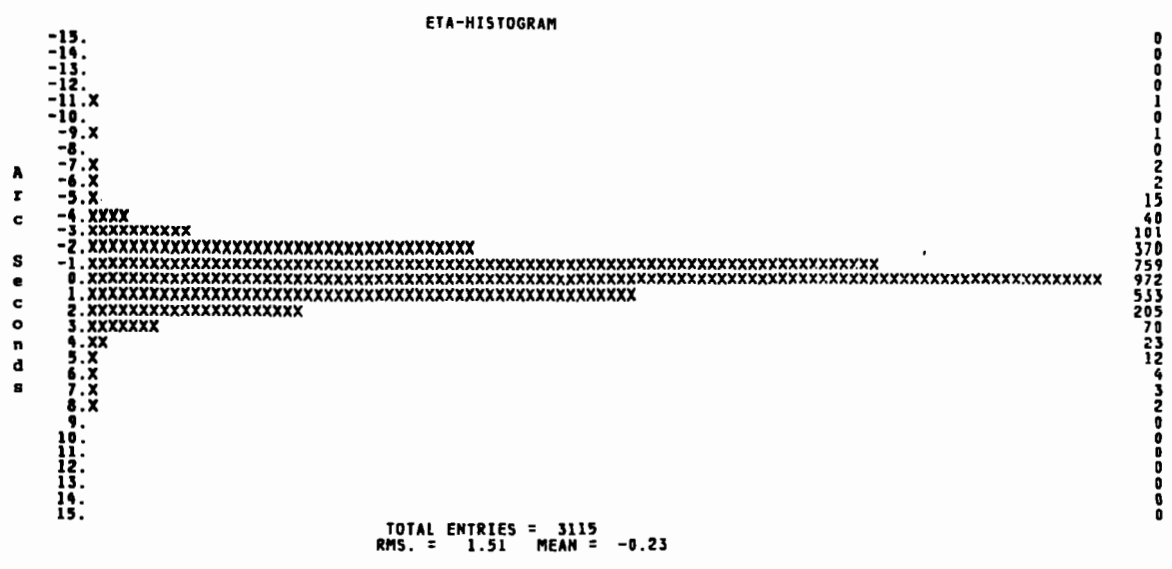


Figure 9. —Distribution of Regional Distortions in the Prime Vertical

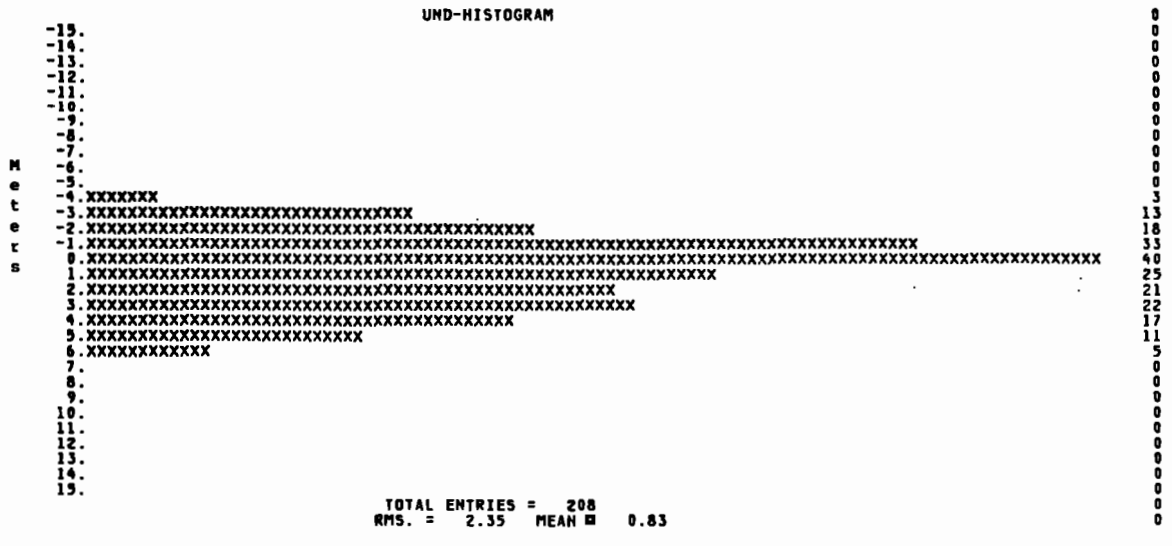


Figure 10. —Distribution of Regional Distortions of Geoid Undulations



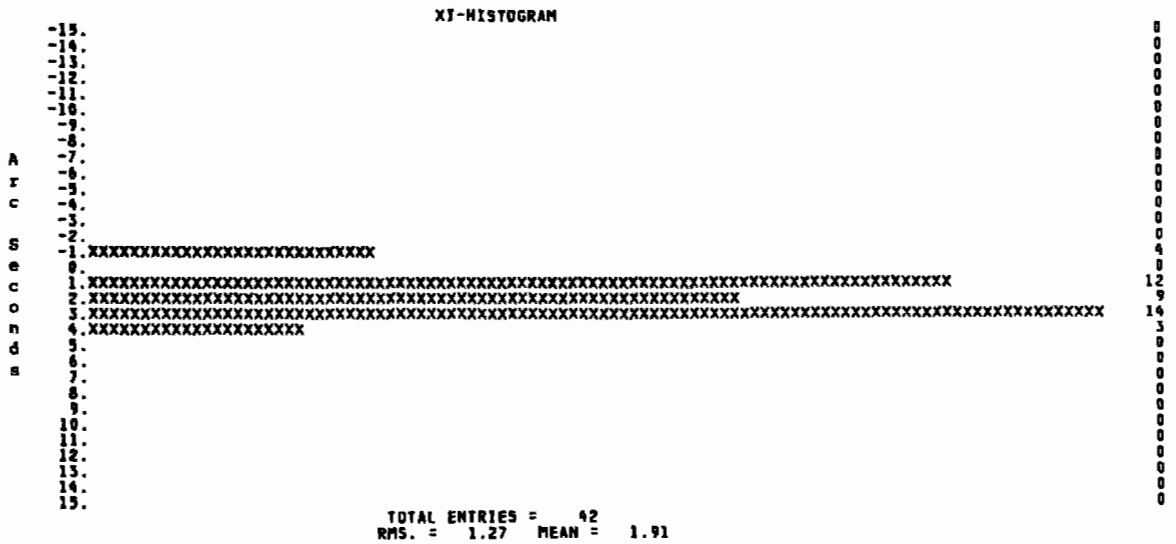


Figure 14. —Distribution of Regional Distortions in the Meridian in area  $\phi=44^\circ - 46^\circ, \lambda=116^\circ - 125^\circ$



Figure 15. —Distribution of Regional Distortions in the Prime Vertical in area  $\phi=44^\circ - 46^\circ, \lambda=116^\circ - 125^\circ$

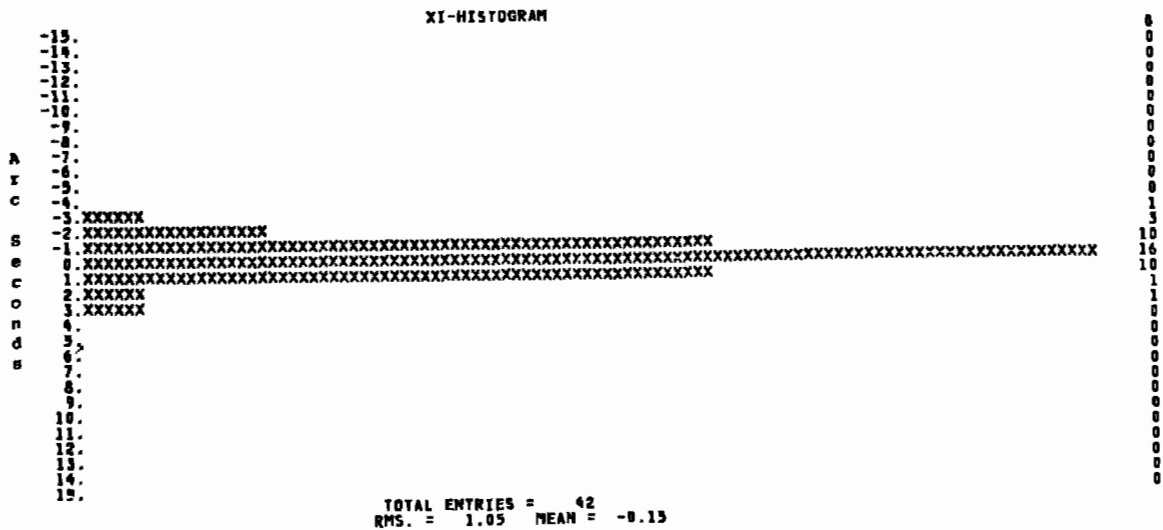


Figure 16. —Distribution of Residual Differences in the Meridian in area  $\phi=44^\circ - 46^\circ, \lambda=116^\circ - 125^\circ$

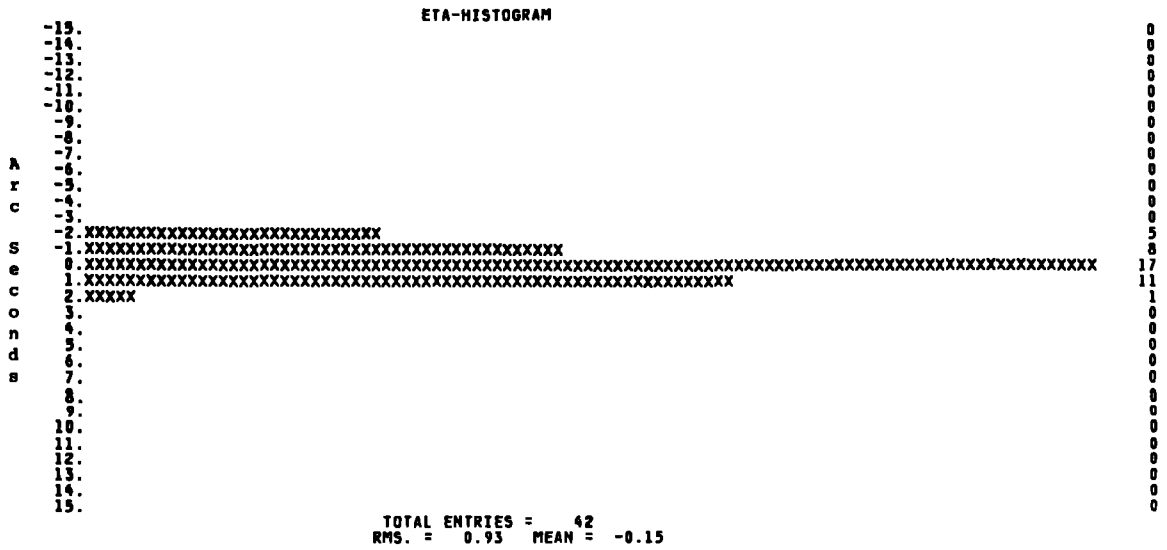


Figure 17. —Distribution of Residual Differences in the Prime Vertical in area  $\phi=44^\circ - 46^\circ, \lambda=116^\circ - 125^\circ$

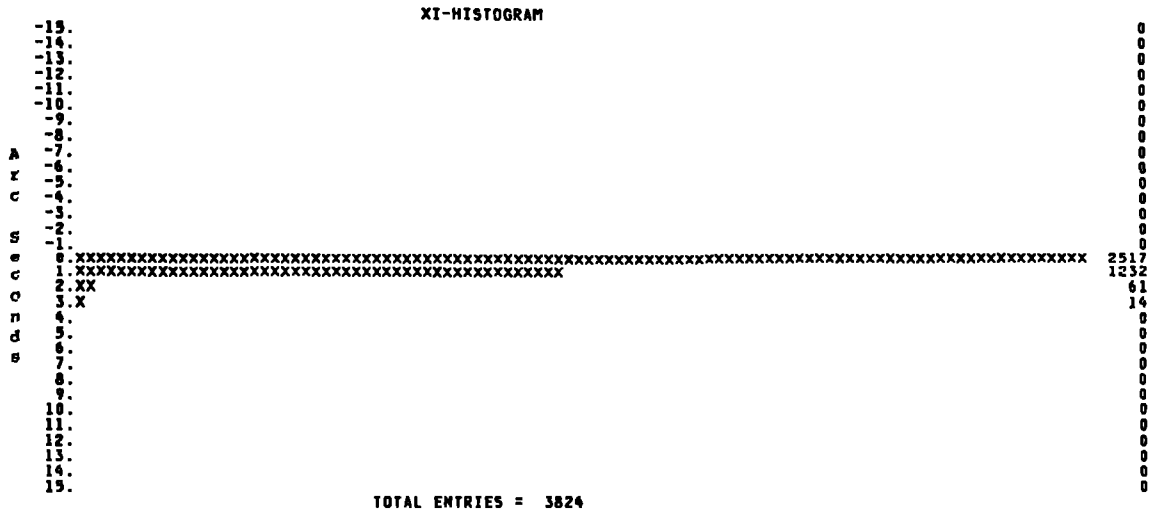


Figure 18. —Distribution of Estimated Sigmas in the Meridian in area  $\phi=44^\circ - 46^\circ, \lambda=116^\circ - 125^\circ$

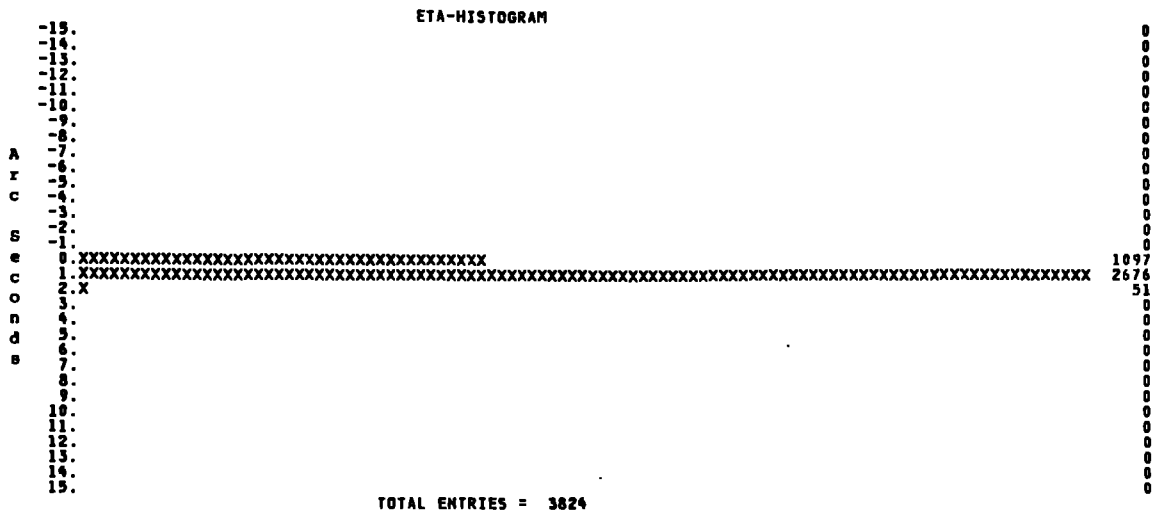


Figure 19. —Distribution of Estimated Sigmas in the Prime Vertical in area  $\phi=44^\circ - 46^\circ, \lambda=116^\circ - 125^\circ$

Table 3. — Calibration values in area  $\phi=44^\circ - 46^\circ, \lambda=116^\circ - 125^\circ$

GRAVIMETRIC PREDICTIONS AT LAPLACE (ASTRO.) STATIONS AND CALIBRATION VALUES  
(TERRAIN CORRECTED (OPTIONAL) ASTRO. DEFLECTIONS)  
NO. OF STATIONS = 65

QID	QSN	LATITUDE		LONGITUDE		H	GEODETIC		GRAVIMETRIC		TRANSFORMS.		CALIBRATION		
		(NORTH)	(WEST)	(WEST)	(WEST)		KSI (N)	ETA (W)	KSI (N)	ETA (W)	KSI (N)	ETA (W)	KSI (N)	ETA (W)	
1	N44117212	1	44. 16.	3.38	117. 3.	8.61	645.10	-6.51	3.22	-5.30	-0.60	-5.96	2.34	-0.55	0.88
2	N44117212	4	44. 17.	4.46	117. 6.	38.50	690.19	-7.26	2.60	-6.07	-0.58	-6.73	2.36	-0.53	0.24
3	N44118314	1	44. 26.	41.54	118. 42.	9.44	1115.97	-3.24	5.67	-1.56	3.32	-2.28	6.38	-0.96	-0.71
4	N44120411	1	44. 54.	52.46	120. 35.	43.57	1316.10	-0.32	1.17	-2.32	-1.10	-3.13	2.09	2.81	-0.92
5	N44120443	2	44. 45.	13.00	120. 52.	44.61	1109.50	4.91	10.93	1.88	6.96	1.06	10.17	3.85	0.76
6	N44121111	1	44. 58.	31.14	121. 4.	47.93	367.60	-3.44	2.64	-6.37	-0.93	-7.20	2.29	3.76	0.35
7	N44121122	1	44. 36.	34.82	121. 2.	50.50	968.30	5.55	13.83	2.89	8.49	2.07	11.71	3.48	2.12
8	N44121123	2	44. 34.	41.97	121. 11.	24.94	771.30	4.10	8.28	2.50	4.51	1.68	7.74	2.42	0.54
9	N44121214	2	44. 28.	51.55	121. 12.	35.81	1196.19	2.71	9.66	0.40	5.65	-0.42	8.88	3.13	0.78
10	N44121232	9	44. 3.	38.52	121. 16.	55.55	1216.39	4.56	3.72	3.02	-0.17	2.21	3.07	2.35	0.65
11	N44121241	3	44. 23.	31.94	121. 17.	42.79	891.30	-0.20	6.12	-1.34	2.71	-2.16	5.95	1.96	0.17
12	N44121242	8	44. 15.	12.04	121. 18.	6.39	1248.60	2.06	4.59	-0.29	0.55	-1.11	3.79	3.17	0.80
13	N44122413	3	44. 45.	49.89	122. 38.	7.83	476.50	0.47	9.72	-0.44	6.30	-1.33	9.63	1.80	0.09
14	N44123144	4	44. 54.	18.68	123. 23.	38.72	349.80	-5.40	-7.67	-5.67	-12.66	-6.59	-9.28	1.19	1.61
15	N44123222	21	44. 3.	29.21	123. 5.	27.23	196.00	-0.94	1.76	0.70	-4.87	-0.19	-1.51	-0.75	3.27
16	N44123223	6	44. 4.	5.80	123. 11.	16.72	116.74	-0.02	-0.45	-0.62	-5.54	-1.51	-2.17	1.49	1.72
17	N44123224	9	44. 11.	36.34	123. 12.	40.37	101.00	-2.55	-1.56	-2.65	-7.41	-3.55	-4.04	1.00	2.48
18	N45116114	3	45. 57.	41.32	116. 10.	54.50	1007.89	4.92	2.81	2.08	-1.19	1.42	1.68	3.50	1.13
19	N45116131	9	45. 44.	36.95	116. 19.	24.36	446.60	1.81	-0.23	1.75	-4.55	1.09	-1.67	0.72	1.44
20	N45116141	1	45. 57.	41.38	116. 17.	51.87	1021.00	-0.56	3.29	-0.84	0.13	-1.50	3.01	0.94	0.28
21	N45116214	4	45. 26.	12.00	116. 9.	44.90	1007.39	-4.39	3.88	-5.14	0.0	-5.79	2.87	1.40	1.01
22	N45116433	2	45. 36.	14.34	116. 58.	54.20	1421.69	4.17	4.39	1.99	-0.35	1.31	2.58	2.86	1.81
23	N45117344	3	45. 26.	23.95	117. 57.	59.69	836.00	1.86	7.66	0.0	3.19	-0.72	6.19	2.58	1.47
24	N45117344	12	45. 24.	22.22	117. 58.	43.30	840.29	0.84	6.31	-0.12	1.30	-0.84	4.30	1.68	2.01
25	N45118212	6	45. 19.	48.35	118. 5.	38.35	849.69	5.01	-1.79	2.91	-6.37	2.19	-3.36	2.82	1.57
26	N45118212	13	45. 19.	50.82	118. 5.	40.20	850.00	5.02	-1.79	2.81	-6.41	2.09	-3.40	2.93	1.61
27	N45119124	1	45. 44.	37.22	119. 11.	19.12	217.00	2.00	7.32	0.24	2.22	-0.53	5.31	2.53	2.01
28	N45119142	2	45. 46.	17.79	119. 17.	47.50	231.10	0.59	4.23	-0.99	0.0	-1.76	3.10	2.35	1.13
29	N45119441	2	45. 59.	44.06	119. 49.	10.98	216.19	-4.29	-0.39	-5.49	-2.63	-6.29	0.51	2.00	-0.90
30	N45119443	3	45. 50.	59.41	119. 56.	21.09	396.69	-4.23	-1.81	-5.93	-5.51	-6.73	-2.37	2.50	0.56
31	N45120121	1	45. 40.	11.22	120. 1.	21.55	276.69	1.17	2.19	0.02	-1.94	-0.78	1.21	1.95	0.98
32	N45120123	6	45. 31.	4.22	120. 9.	32.43	437.19	5.66	4.47	2.92	1.12	2.12	4.28	3.54	0.19
33	N45120213	1	45. 22.	11.56	120. 12.	14.81	831.50	6.16	5.29	3.86	2.16	3.06	5.32	3.10	-0.03
34	N45120231	1	45. 14.	18.96	120. 17.	42.26	1017.39	2.63	4.15	0.18	0.17	-0.62	3.34	3.25	0.81
35	N45120233	1	45. 5.	56.64	120. 24.	4.42	887.60	2.70	6.13	0.60	2.75	-0.20	5.93	2.90	0.20
36	N45121111	2	45. 59.	27.70	121. 4.	57.59	1148.00	-3.25	8.35	-3.16	6.52	-4.01	9.74	0.76	-1.39
37	N45121331	1	45. 14.	20.76	121. 48.	47.59	1432.39	-5.64	6.91	-6.05	5.22	-6.91	8.49	1.27	-1.58
38	N45122312	11	45. 20.	33.71	122. 31.	10.81	200.10	-1.48	2.43	-1.18	-0.85	-2.08	2.47	0.60	-0.04
39	N45122422	88	45. 32.	48.75	122. 33.	53.06	185.30	-0.41	4.21	-1.48	-0.96	-2.38	2.37	1.97	1.84
40	N45122423	3	45. 31.	7.72	122. 40.	38.50	17.00	0.56	3.00	-0.02	-2.31	-0.93	1.02	1.49	1.98
41	N45123224	33	45. 14.	48.65	123. 13.	16.63	98.89	-4.53	-9.12	-4.18	-12.84	-5.10	-9.47	0.57	0.35
42	N45123341	12	45. 28.	33.93	123. 50.	34.36	5.26	-3.16	23.22	-2.78	17.36	-3.73	20.77	0.57	2.45

16

Table 4. —Residual Differences in area  $\phi=44^\circ - 46^\circ, \lambda=116^\circ - 125^\circ$

GRAVIMETRIC PREDICTIONS AT LAPLACE STATIONS WITH CALIBRATIONS FROM  
10 NEIGHBOURING STATIONS (TERRAIN CORRECTED (OPTIONAL)  
AND ERROR ANALYSIS)

QID	QSN	OBS.		PRED.		V		
		KSI (N)	ETA (W)	KSI (N)	ETA (W)	KSI (N)	ETA (W)	
1	N44117212	1	-6.51	3.22	-6.45	2.59	-0.06	0.63
2	N44117212	4	-7.26	2.60	-7.25	3.25	-0.01	-0.65
3	N44118314	1	-3.24	5.67	-0.11	7.72	-3.13	-2.05
4	N44120411	1	-0.32	1.17	0.13	2.65	-0.45	-1.48
5	N44120443	2	4.91	10.93	4.20	10.96	0.71	-0.03
6	N44121111	1	-3.44	2.64	-4.10	2.94	0.66	-0.30
7	N44121122	1	5.55	13.83	4.97	12.27	0.58	1.56
8	N44121123	2	4.10	8.28	4.78	8.72	-0.68	-0.44
9	N44121214	2	2.71	9.66	2.09	9.48	0.62	0.18
10	N44121232	9	4.56	3.72	5.13	3.74	-0.57	-0.02
11	N44121241	3	-0.20	6.12	0.87	6.73	-1.07	-0.61
12	N44121242	8	2.06	4.59	1.29	4.27	0.77	0.32
13	N44122413	3	0.47	9.72	-0.34	10.83	0.81	-1.11
14	N44123144	4	-5.40	-7.67	-5.74	-8.11	0.34	0.44
15	N44123222	21	-0.94	1.76	1.19	0.34	-2.13	1.42
16	N44123223	6	-0.02	-0.45	-1.57	0.74	1.55	-1.19
17	N44123224	9	-2.55	-1.56	-2.76	-1.90	0.21	0.34
18	N45116114	3	4.92	2.81	2.38	2.21	2.54	0.60
19	N45116131	9	1.81	-0.23	3.00	-0.89	-1.19	0.66
20	N45116141	1	-0.56	3.29	1.31	4.21	-1.87	-0.92
21	N45116214	4	-4.39	3.88	-4.29	4.04	-0.10	-0.16
22	N45116433	2	4.17	4.39	2.88	3.74	1.29	0.65
23	N45117344	3	1.86	7.66	1.06	8.16	0.80	-0.50
24	N45117344	12	0.84	6.31	1.77	5.78	-0.93	0.53
25	N45118212	6	5.01	-1.79	5.12	-1.75	-0.11	-0.04
26	N45118212	13	5.02	-1.79	4.91	-1.83	0.11	0.04
27	N45119124	1	2.00	7.32	1.84	6.37	0.16	0.95
28	N45119142	2	0.59	4.23	0.77	4.88	-0.18	-0.65
29	N45119441	2	-4.29	-0.39	-3.78	1.14	-0.51	-1.53
30	N45119443	3	-4.23	-1.81	-4.49	-2.27	0.26	0.46
31	N45120121	1	1.17	2.19	2.10	1.46	-0.93	0.73
32	N45120123	6	5.66	4.47	4.82	4.63	0.84	-0.16
33	N45120213	1	6.16	5.29	6.24	5.78	-0.08	-0.49
34	N45120231	1	2.63	4.15	2.40	3.44	0.23	0.71
35	N45120233	1	2.70	6.13	2.94	6.26	-0.24	-0.13
36	N45121111	2	-3.25	8.35	-1.12	9.86	-2.13	-1.51
37	N45121331	1	-5.64	6.91	-4.81	9.15	-0.83	-2.24
38	N45122312	11	-1.48	2.43	-0.44	4.10	-1.04	-1.67
39	N45122422	88	-0.41	4.21	-1.13	3.79	0.72	0.42
40	N45122423	3	0.56	3.00	0.72	2.43	-0.16	0.57
41	N45123224	33	-4.53	-9.12	-3.94	-7.97	-0.59	-1.15
42	N45123341	12	-3.16	23.22	-2.72	21.91	-0.44	1.31

MINIMUM PREDICTION DISTANCE 0.1 MIN.  
MAXIMUM PREDICTION DISTANCE 122.6 MIN.  
AVERAGE PREDICTION DISTANCE 61.4 MIN.

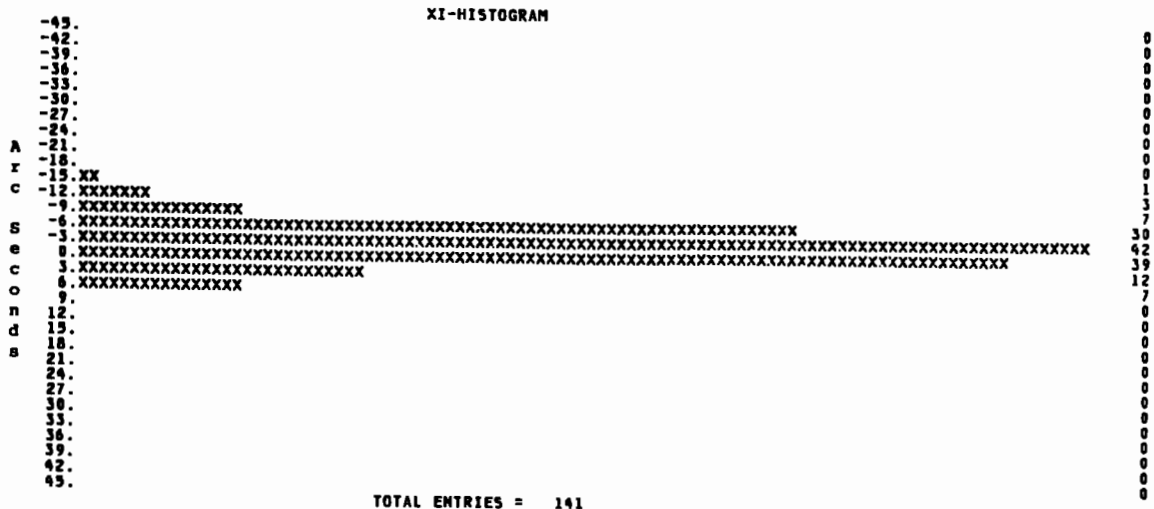


Figure 20. —Distribution of Astronomic Deflections in the Meridian in area  $\phi=39^\circ - 44^\circ, \lambda=116^\circ - 125^\circ$



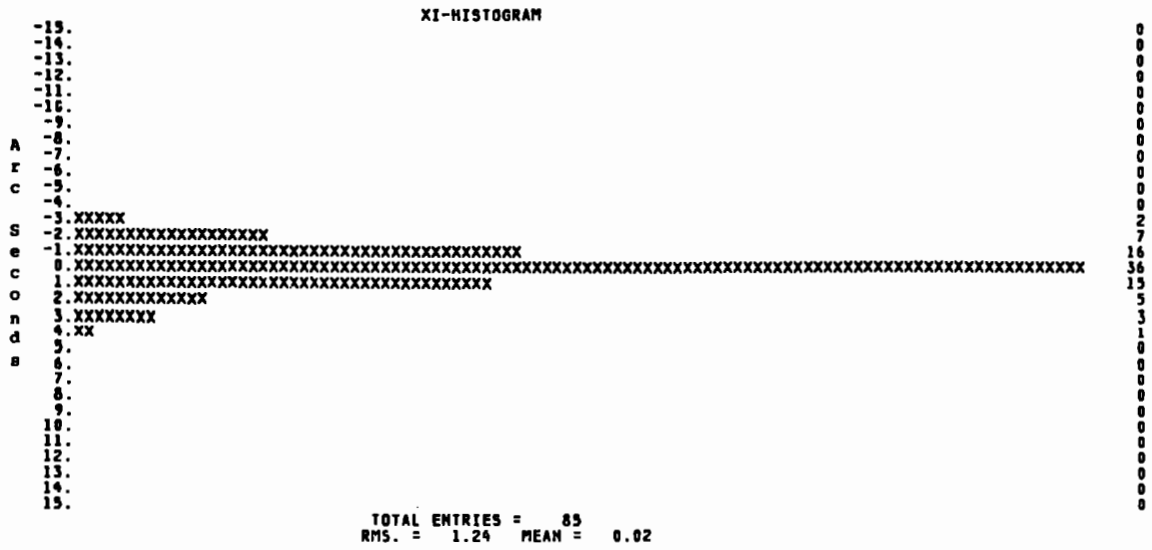


Figure 24. —Distribution of Residual Differences in Meridian in area  $\phi=39^\circ - 44^\circ, \lambda=116^\circ - 125^\circ$

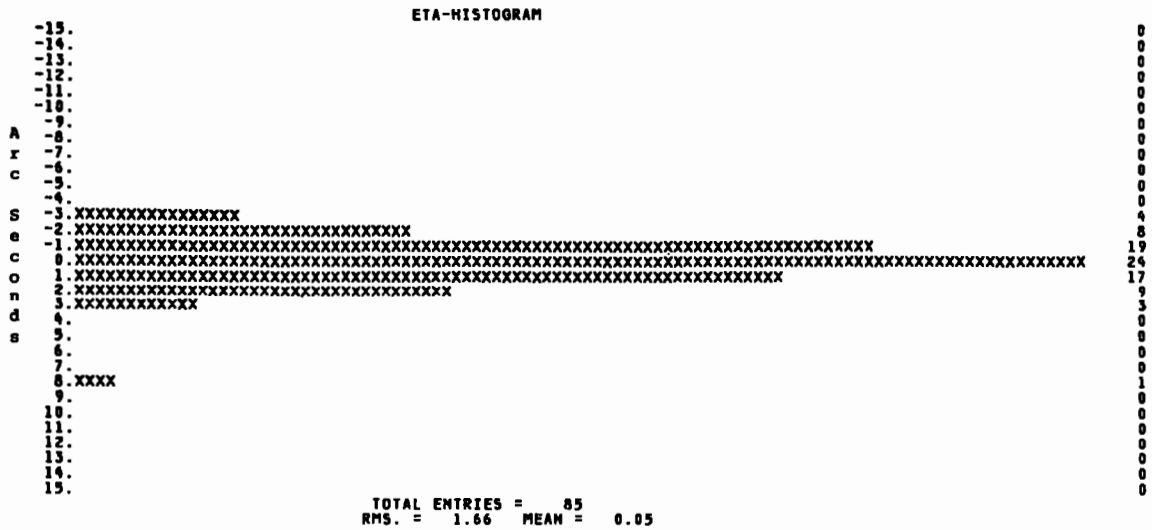


Figure 25. —Distribution of Residual Differences in the Prime Vertical at area  $\phi=39^\circ - 44^\circ, \lambda=116^\circ - 125^\circ$

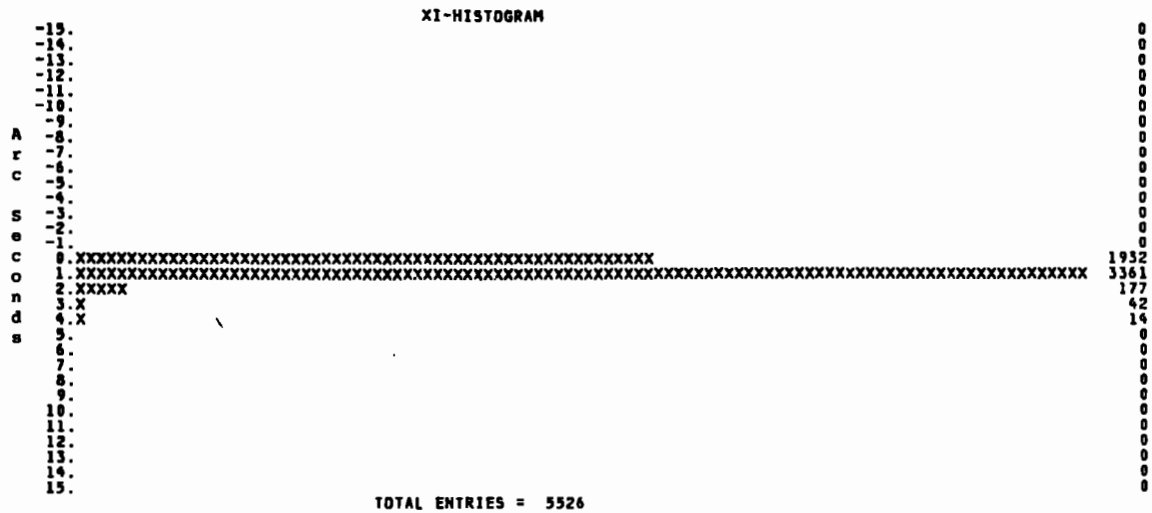


Figure 26. —Distribution of Preliminary Estimated Prediction Errors in the Meridian at area  $\phi=39^\circ - 44^\circ, \lambda=116^\circ - 125^\circ$







# BIBLIOGRAPHY

- Alger, D. E., 1981: The design, development, and implementation of the National Geodetic Survey data base query system, *Proceedings of the International Symposium: Management of Geodetic Data*, Copenhagen, Denmark.
- Alger, D. E., 1978: Implementation of the National Geodetic Survey data base, *Second International Symposium on Problems Related to the Redefinition of North American Geodetic Networks*, April 24-28, Arlington, Va.
- Bjerhammar, A., 1967: On the theory of a new geoid, USAEGIMRADA, Research Institute for Geodetic Sciences.
- Bossler, J. D., 1978: Status of the new adjustment in the United States, *Proceedings of the Second International Symposium on Problems Related to the Redefinition of the North American Geodetic Networks*, April 24-28, Arlington, Va.
- Chin, M., 1981: Estimation of Local Gravity Anomaly Covariance Functions. Presented at Fall Meeting of the American Geophysical Union, San Francisco, Calif., December 1981.
- Dimitrijevič, I. J., 1972: The Use of Terrain Corrections in Computing Gravimetric Deflection of the Vertical Components and Geoid Heights. Presented at 53rd Annual Meeting of American Geophysical Union, April, Washington, D.C.
- Fell, P. and Karaska, M., 1981: Decreasing the influence of distant zones with modification to the Stokes and Vening-Meinesz Kernels, NSWC TR 80-350, Naval Surface Weapons Center.
- Franke, R., 1979: A critical comparison of some methods for interpolation of scattered data, *Report NPS-53-79-003*, Naval Postgraduate School, Monterey, Calif.
- Fury, R. J., 1981: Data bank techniques for the management of large-volume geodetic and geophysical data at the National Geodetic Survey, *Proceedings of the International Symposium: Management of Geodetic Data*, Copenhagen, Denmark.
- Goad, C. C., 1981: Local Geoid Interpolation. Presented at Fall Meeting of the American Geophysical Union, December, San Francisco, Calif.
- Groten, E., 1981: Determination of plumb line curvatures by astronomical and gravimetric methods, *NOAA Technical Memorandum NOS NGS 30*, 17 pp.
- Hagiwara, Y., 1973: Truncation error formulas for the geoidal height and the deflection of the vertical, *Bulletin Geodesique*, No. 106.
- Hein, G. W. and Lenze, K., 1979: On the Accuracy and Economy of Various Interpolation and Prediction Methods, Institute für Physikalische Geodäsie, Technische Hochschule, Federal Republic of Germany. Technical translation, DMAAC, 1979.
- Heiskanen, W. A. and Moritz, H.: *Physical Geodesy*, W.H. Freeman and Company, 1967.
- Hopkins, J. and McEntee, D., 1974: GEOSYNOPSIS (UEG273)-ULB522, User's Guide, Air Force Cartographic and Information Center, St. Louis, Mo.
- Lachapelle, G., 1978: Evaluation of  $1^\circ \times 1^\circ$  mean free-air gravity anomalies in North America, Geodetic Survey Division, Geodetic Survey of Canada, Ottawa.
- Moritz, H., 1968: On the use of the terrain correction in solving Molodensky's Problem, *Report No. 108*, The Ohio State University Research Foundation.
- Pickrell, A. J., 1979: *Representation of Hydrographic Surveys and Ocean Bottom Topography by Analytical Models*, M.S. Thesis, Naval Postgraduate School, Monterey, Calif.
- Rice, D. A., 1952: Deflections of the vertical from gravity anomalies, *Bulletin Geodesique*, 51 (2), 105-118.
- Schwarz, C. R., 1978: Deflection computations for network adjustment in the United States, *Proceedings of the Second International Symposium on Problems Related to the Redefinition of North American Geodetic Network*, April 24-28, Arlington, Va.
- Shultz, M., Scheile, D., Widitz, F. and McEntee, D., 1974: INNERING (UEG273) ULB522, User's Guide, Air Force Cartographic and Information Center, St. Louis, Mo.
- Strange, W. E. and Fury, R. J., 1977: Computation of deflections of the vertical in support of the readjustment of the North American Datum, *Proceedings of the International Symposium on Optimization of Design and Computation of Control Networks*, Sopron, Hungary.
- Tscherning, C. C., 1975: Application of collocation for the planning of gravity surveys, *Bulletin Geodesique*, No. 116.
- Vincenty, T., 1976: Determination of North American Datum 1983 coordinates of map corners, *NOAA Technical Memorandum NOS NGS-6*, 8 pp.

# APPENDIX A

## Recursive Relations of Legendre Functions

Derived recursion relations of normalized Legendre functions:

$$\bar{P}_n^o(\sin\phi) = \frac{\sqrt{2n+1}}{n} \left\{ \sqrt{2n-1} \sin\phi \bar{P}_{n-1}^o(\sin\phi) - (n-1) \sqrt{\frac{1}{2n-3}} \bar{P}_{n-2}^o(\sin\phi) \right\}$$

$$\bar{P}_n^m(\sin\phi) = \sqrt{\frac{2n+1}{(n+m)(n+m-1)}} \left\{ \sqrt{\delta(2n-1)} \left[ \cos\phi \bar{P}_{n-1}^{m-1}(\sin\phi) + \sqrt{\frac{(n-m)(n-m-1)}{2n-3}} \bar{P}_{n-2}^m(\sin\phi) \right] \right\}$$

Derived recursion relations of derivatives of normalized Legendre functions:

$$\frac{d\bar{P}_n^o(\sin\phi)}{d\phi} = \sqrt{\frac{2n+1}{n}} \left\{ \sqrt{2n-1} \left[ \sin\phi d\bar{P}_{n-1}^o(\sin\phi) + \cos\phi \bar{P}_{n-1}^o(\sin\phi) \right] - (n-1) \sqrt{\frac{1}{2n-3}} d\bar{P}_{n-2}^o(\sin\phi) \right\}$$

$$\frac{d\bar{P}_n^m(\sin\phi)}{d\phi} = \sqrt{\frac{2n+1}{(n+m)(n+m-1)}} \left\{ \sqrt{\delta(2n-1)} \left[ \cos\phi d\bar{P}_{n-1}^{m-1}(\sin\phi) - \sin\phi \bar{P}_{n-1}^{m-1}(\sin\phi) \right] + \sqrt{\frac{(n-m)(n-m-1)}{2n-3}} d\bar{P}_{n-2}^m(\sin\phi) \right\}$$

when  $(m-1) > 0$ , then  $\delta=1$ , when  $(m-1)=0$ , then  $\delta=2$ ; the functions are zero by definition when  $n=2$ ,  $n=1$ ,  $m=1 \leq 0$ .

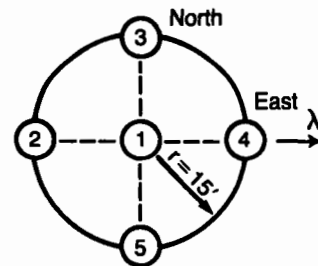
## APPENDIX B

### Linear Interpolation of Global Component of Gravity on the Geoid

Values of  $\Delta g^o$  (equation 11) are obtained by spherical harmonic series at the network station (1), and at symmetrically located four points (i.e., 2, 3, 4, 5). Any other values of  $\Delta g^o(\phi, \lambda)$  in the station's vicinity are obtained by linear interpolation:

$$\Delta g^o(\phi, \lambda) = \frac{\Delta g^o(3) - \Delta g^o(5)}{2r} \phi' + \frac{\Delta g^o(2) - \Delta g^o(4)}{2r} \lambda' + \Delta g^o(B1)$$

where  $\phi'$  and  $\lambda'$  are geodetic positions, and  $r$  is the distance of symmetrically located points from network station in arc minutes.



Anomaly Computation Points on the Geoid

# APPENDIX C

## Geodetic Reference System of 1980

$$GM = 3.986005 \times 10^{14} \text{ cm}^3/\text{sec}^2$$

$$a = 6378137 \text{ meters}$$

$$J_2 = 1082.63 \times 10^{-6}$$

$$\omega = 0.7292115 \times 10^{-4} \text{ rads/sec}$$

$$1/f = 298.2572221(*)$$

(\*) Derived

# APPENDIX D

## Topographic Height Interpolation

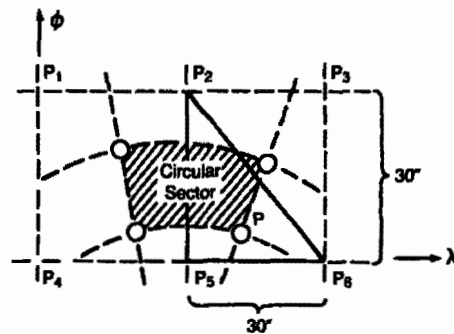
Topographic heights of circular sector corners were computed via three-point interpolation from evenly distributed ( $P_1, P_2, \dots, P_6$ ) digitized elevations in the NGS data bank. The point elevation  $h_P$  of sector corner  $P$  is interpolated from values at geographic grid intersections  $P_2, P_5,$  and  $P_6$  where

$$h_P = Ah_{P_6} + Bh_{P_5} + Ch_{P_2}$$

$$A = 1 + (\phi_{P_5} - \phi_{P_2})(\lambda_P - \lambda_{P_6})(\lambda_{P_5} - \lambda_{P_2})(\phi_P - \phi_{P_6})$$

$$B = 1 + (\phi_{P_2} - \phi_{P_6})(\lambda_P - \lambda_{P_5})(\lambda_{P_2} - \lambda_{P_6})(\phi_P - \phi_{P_5})$$

$$C = 1 + (\phi_{P_6} - \phi_{P_5})(\lambda_P - \lambda_{P_2})(\lambda_{P_6} - \lambda_{P_5})(\phi_P - \phi_{P_2})$$



Topographic Height Interpolation

U.S. GOVERNMENT PRINTING OFFICE: 1984 - 421-009 - 227/719

**U.S. DEPARTMENT OF COMMERCE**  
**National Oceanic and Atmospheric Administration**  
**National Ocean Service**  
**Charting and Geodetic Services**  
**National Geodetic Survey, N/CG17X2**  
**Rockville, Maryland 20852**

---

**OFFICIAL BUSINESS**  
**LETTER MAIL**

**POSTAGE AND FEES PAID**  
**U.S. DEPARTMENT OF COMMERCE**  
**COM-210**  
**THIRD CLASS**

